Chemical and electrical diagnosis of two configurations of dielectric barrier discharges applied to nitric oxides degradation

Estrada Martínez N., Valdivia Barrientos R. [1], Pacheco Sotelo J. [1],
García Estrada R. y Garduño Aparicio M.
Instituto Tecnológico de Toluca

Pacheco Pacheco M. y Rivera Rodríguez C.
Instituto Nacional de Investigaciones Nucleares

The distinctive of non-thermal plasma (NTP) techniques is the efficient use of electrical energy through selective decomposition of the pollutant molecules. NTP processes can simultaneously treat several pollutants at atmospheric pressure with a quite good efficiency at relatively low energy consumption. In this work, NTP was used to remove nitric oxides from a mixture of air, water vapor and helium. Non thermal plasma was generated by dielectric barrier discharge at atmosphere pressure. In this work two different configurations were employed for the process: single dielectric barrier discharge (DBD) and double dielectric barrier discharge (2DBD). The aim of this work is to determine which configuration is most suitable for NOx treatment. A chemical model was developed to observe the species behavior in the plasma and results of numerical simulation demonstrated a good agreement with experimental data of the removal process, achieving more than 96% of NOx removal efficiency. From an electrical diagnosis several experimental parameters such as power, frequency, initial concentration of NOx and specific input energy were tested.
To determine the electronic temperature and electronic densities in the plasma, an optical emission spectroscopy study was accomplished.

Keywords: Non-thermal plasma; Dielectric barrier discharge; Nitric oxides degradation; Removal process

1. Introduction

Nitric oxides contribute to photochemical smog and acid rain; these pollutants affect vegetation, buildings and human health [1]. Non-thermal plasma technologies have been used in toxic gas removal [2], because most of the electrical energy input is transferred into electron kinetic energy forming highly chemically active compounds, these active compounds are very efficient in the NOx treatment [3]. The purpose of NTP is to create radicals through electron impact, dissociation and ionization of the molecules in the effluent gas.

Dielectric barrier discharges are characterized by the presence of one or more insulating layers in the current path between metal electrodes in addition to the discharge gap(s) [4]. Dielectric barrier discharge reactor with two arrangements is depicted. Both configurations were experimentally and theoretically analyzed, in order to conclude which of them is better for NOx removal.

2. Fundamental Concepts

Kinetic model used to symbolize NOx treatment was developed in two phases. The first phase was to the formation of streamer head with high electric field values at 1×10^{-8} s with initial electron density of 1 cm^{-3} [5]. In this phase two mechanisms for active species formation were considered: dissociation by direct electron impact with gas molecules and quenching of the excited states such as O(^{1}D) and N$_2$(A). Some primary radicals (OH$^\bullet$, O$^\bullet$, N$^\bullet$) appear during this phase. The radicals production

is supposed uniformly distributed within the whole volume. The second phase was the formation of a streamer channel which is connected to the streamer head. In this phase NOx react with active species.

The reaction mechanism of NOx degradation is shown in figure 1, rate coefficients were used at an electric field of 40 Td for single DBD and 13 Td for 2DBD [6, 7].

The model takes into account twenty two chemical species (e$^-$, N$_2$, O$_2$, H$_2$O, O$^\bullet$, N$^\bullet$, OH$^\bullet$, H$^\bullet$, O$_2$(a$^1 \Delta$ g), O(^{1}D), N$_2$(A), O$^-_2$, O$^-$, O$^+_2$, H$^-$, O$_3$, NO$_2$, NO$_3$, N$_2$O$_5$, N$_2$O, HNO$_3$, HNO$_2$), and 76 chemical reactions [2, 6]. Reaction rate coefficients involving electrons and neutral species were taken from [3, 5].

The model considers a mass balance of the chemical species mentioned above. The kinetic differential equations are solved by a variable order method based on numerical differentiation formulae [8].

The spectroscopic measurements are based on relative line intensities of either the same atom. The method employed to calculate electron temperature was Boltzmann plot [9]; the spectral lines data were obtained from NIST [10]. To determine the electron density, the relationship between intensities of two lines was applied [11].
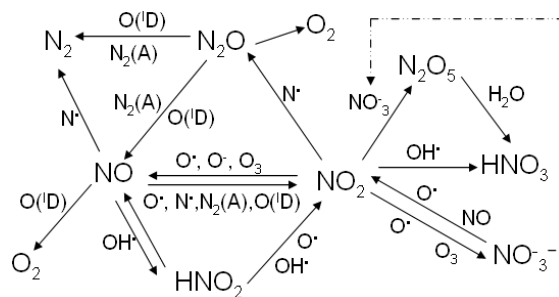
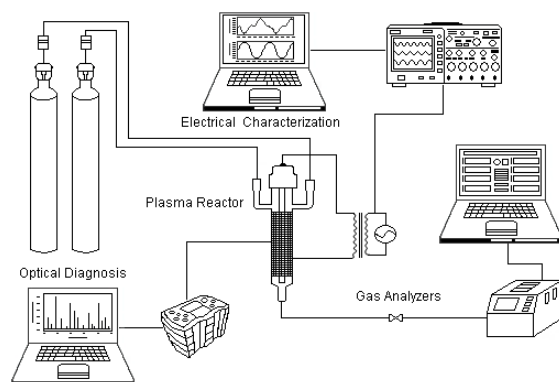**Figure 1.** Reaction mechanism of NOx degradation.
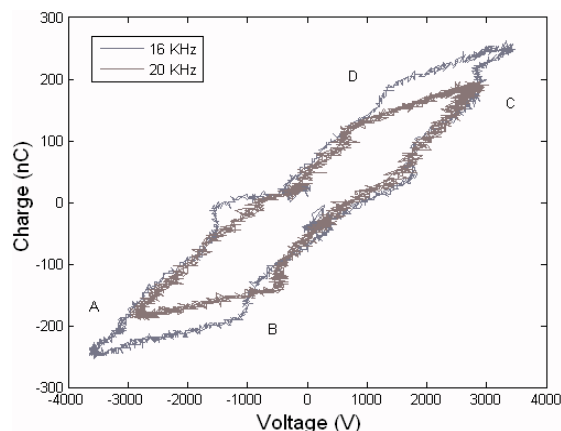

Figure 2. Experimental system.

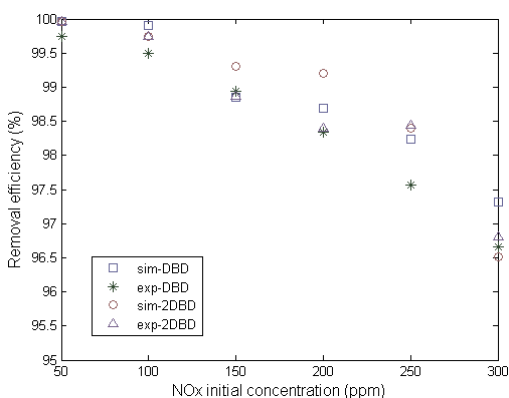**Figure 3.** Lissajous figures of NOx degradation.

Figure 4. Experimental and simulation removal efficiency.

3. Experimental SET – UP

The experimental system used in degradation process is shown in figure 2; it is composed of a dielectric barrier discharge reactor which could be DBD or 2DBD, the alternating current power supply to ignite NTP, was developed in our laboratory, the operation and design are described by Valdivia [12]. The system was equipped for analysis and monitoring of gases in order to determine chemical diagnosis, the oscilloscope, high voltage probe, current probe and capacitor were employed to determine electrical diagnosis, for optical diagnostics a digital spectrometer (Jaz Ocean Optics) was used, the digital spectrometer enables an optical resolution of 0.3 nm (FWHM) covering from 200 nm to 1100 nm. Dielectric barrier discharge reactors work at atmospheric pressure of 0.73 atm (the laboratory is situated at 3100 meters above sea level) and at room temperature of 289 K. The schematic of the reactor consists in a tube of pyrex glass with an internal radius of 11.1 mm, a length of 75 mm and a thickness of 1.2 mm; a stainless steel concentric central electrode of radius of 2.54 mm is set inside the pyrex tube, for 2DBD a tube of alumina wraps the central electrode; a metallic mesh, covering the pyrex tube, plays the role of the external electrode.

NOx were mixed with air, water vapor and helium before its entrance to the reactor. To obtain the OH$^{\cdot}$ radicals necessary for NOx removal treatment, a 5%vol. of H_2O was added to the system, which was took of the humid air, in our case water vapor was considered like humidity. Several concentrations of NOx (50–300 ppm) were tested. Outlet gases were measured with a PG–250 Horiba analyzer; it employs chemiluminescence for NOx detection. When NTP was ignited, degradation process began, the formation of microdischarge head was around 1 ns, it gave rise to the formation of active species, subsequently these species react with nitrogen oxides following reaction mechanism proposed above (figure 1).

4. Results and Discussion

4.1. Electrical Diagnosis

In the following section the electrical diagnosis applied during NOx degradation by DBD and 2DBD is detailed. A simple and reliable method to obtaining power consumed is using Manley's formula and Lissajous figure [13], obtained when plotting the transported electric charge (*Q*) through the discharge as a function of the applied voltage (*V*) [14]. Lissajous figure obtained during NOx degradation in a 2DBD is showed in figure 3. Experimentally, the charge is delivered from the voltage drop across a measuring serial capacitor of 0.111 µF. Specific input energy (*SIE*) indicates the amount of energy needed to remove a given NOx concentration at a given feed flow.

The power applied (*PA*), consumed (*PC*), power efficiency (*PE*), initial concentration (*IC*), specific input

Table 1. Operating conditions in DBD.

I_C (ppm)	Power (W)		R_{NOx} (%)	P_E (%)	SIE (J/l)
	P_A	P_C			
50	19.68	16.44	99.74	83.52	394.48
100	22.08	18.14	99.50	82.15	435.33
150	23.76	19.59	98.94	82.46	470.22
200	24.00	20.00	98.34	83.34	480.04
250	24.00	20.18	97.57	84.11	484.32
300	23.76	20.15	96.66	84.82	483.60

Table 2. Operating conditions in 2DBD.

I_C (ppm)	Power (W)		R_{NOx} (%)	P_E (%)	SIE (J/l)
	P_A	P_C			
50	20.16	16.81	99.97	83.36	403.33
100	21.36	17.91	99.90	83.86	429.90
150	21.60	18.07	98.85	83.66	433.69
200	21.60	18.18	98.69	84.17	436.32
250	21.60	18.29	98.24	84.68	438.98
300	21.60	18.28	97.31	84.61	438.62

energy (*SIE*) and degradation rates (R_{NOx}) achieved in a DBD and in a 2DBD at 1 minute of time are respectively shown in tables 1 and 2, keeping constant the operating frequency. It is important to note the capability of both configurations to treat NOx; however in terms of removal efficiency and power applied, a DBD is more suitable. The coating of the central electrode in 2DBD allows the accumulation of electrons in the dielectric barrier and contributes to diminish the input power [15]. From tables 1 and 2, it is observed that power consumption increases when NOx initial concentration is higher, but the removal percentage decreased. It could be explained by the fact that at higher initial concentration, the amount of radicals consumed increases, so, it is necessary to add higher amount of water in order to increase the amount of radicals.

4.2. Simulation: NO$_x$ removal process

Results obtained from simulation permit to explain the removal process as follows: during first nanoseconds, the energetic electrons created, collide with neutral molecules (N_2, O_2, H_2O) appearing primary radicals ($OH^{\bullet}$, $O^{\bullet}$, $N^{\bullet}$), ions and excited molecules, they react to form radicals by rapid quenching.

NOx removal is controlled mainly by oxidation reactions. The role of $O^{\bullet}$ radical was the oxidation of NO to NO_2. NO and NO_2 could be removed by the $OH^{\bullet}$ radical to form HNO_2 and HNO_3, respectively, but also NO can be reduced by $N^{\bullet}$ radical [16]. The removal process began when NTP was ignited and it is finished when the concentration of species produced during NOx removal remains constant. In terms of removal efficiency (figure 4), a relatively good correlation, between

simulation and experimental results, is observed with DBD (99.52%) and 2DBD (99.80%) at the same time. These removal percentages (Figure 4) were obtained after 1 minute of treatment. Results from the simulation allowed us to observe that densities of $O^{\bullet}$, $OH^{\bullet}$ and $N^{\bullet}$ are close to 10^{15} particles cm^{-3} at about 1 ns for DBD and 2DBD; after that, an exceptionally fast diminution of the concentrations is observed (less of 0.1 µs). Therefore, the formation of radicals occurs on short time scales compared with the subsequent chemical reactions responsible for NOx removal. In figures 5 and 6, the removal process can be observed in parts per million. For NOx removal in DBD, a rapid conversion of NO to NO_2 is obtained, nevertheless the diminution of NOx (NO + NO_2 + N_2O_5 + N_2O) is slower. For NOx removal in 2DBD (figure 6) the conversion of NO to NO_2 is slower than that observed in a DBD; nevertheless the diminution of NOx is faster than DBD. From the simulation, the acids production (HNO_2 and HNO_3) in a DBD is around 20% higher than in a 2DBD. The influence of a double barrier was reflected experimentally in a greater homogeneity in the discharge [17].

The DBD is more efficient to generate $N^{\bullet}$ species, whereas the 2DBD was more effective to produce $O^{\bullet}$ species [6]; it is consistent with results showed in figure 4, because $O^{\bullet}$ radical has greater influence in nitric oxides degradation [6, 9] and 2DBD shown higher removal percentage than DBD.

4.3. Optical emission spectroscopy (OES)

Boltzmann plot was used to calculate electron temperature, the lines employed for DBD were 335.45, 356.31, 381.96, 388.86 nm, and the spectral lines for 2DBD were 335.45, 355.45, 358.73, 392.65 nm. In both cases all lines are representative of the excited helium (He I). The spectral lines employed to calculate electron density (n_e) were 335.45 and 388.865 nm for DBD and 335.45 nm and 358.79 nm for 2DBD. The temperatures and electron densities obtained are shown in table 3.

In 2DBD the power was slightly larger, and then, the electron temperature is higher in 2DBD than in DBD [18]. The duration of microdischarges in DBD is around 50 ns and in 2DBD is 10 ns [19], so 2DBD is more reactive than DBD because the streamer phase is more frequently, for that reason the electrons could be more energized in 2DBD compared with the DBD. Moreover a power increase in 2DBD leads to the generation of a larger number of microdischarges per unit time [18]. The duration of microdischarges could explain an increase in the electron density when a second dielectric barrier is used in the reactor.

Table 3. OES Results.

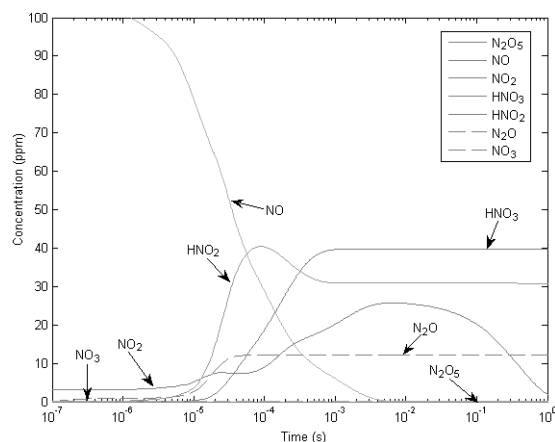| Reactor	Te (eV)	n_e (cm^{-3})
DBD	1.73	6.68 x 10^{14}
2DBD	2.22	29.9 x 10^{14}

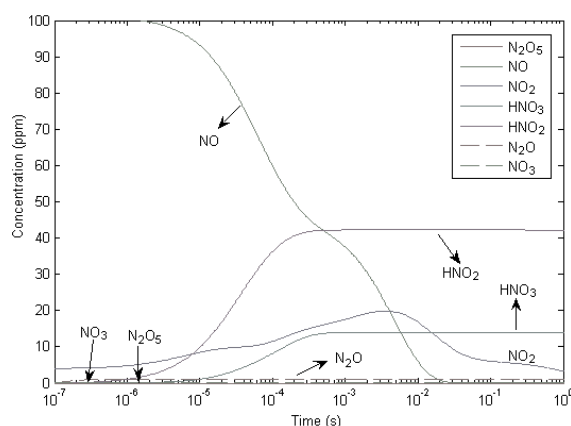**Figure 5.** Simulation of NOx removal in DBD.

Figure 6. Simulation of NOx removal in 2DBD.

5. Conclusions

Removal efficiency was similar in DBD and in 2DBD. In both configurations more than 96% removal percentage were obtained, with less than 25 watts at atmospheric pressure.

Based on simulation results, electrical, chemical and optical diagnosis we can to conclude that 2DBD was the most suitable option in NOx treatment.

References

[1].   Ferrís I, Tortajada J, García I, Castell J, López A, Journal Specialist Pediatric, **57**, 213, (2001).
[2].   Chang J. S, IOP Physics Reviews, No.3, Vol. 2, 2001, 571–574
[3].   Lowke J, Morrow R, IEEE Transactions on Plasma Science, **23**, 661 (1995).
[4].   Kogelschatz U, ABB Corporate Research Ltd, Baden, Switzerland, **5**, 5405 (2000).
[5].   Kim Y, Woo S, Hong S, Young H, IEEE Transactions on Plasma Science, **22**, 305 (2000).
[6].   Pacheco M, Pacheco J, Moreno H, Diaz J, Mercado A, Yousfi M, Plasma Science and Technology, **9**, 682 (2007).
[7].   Valdivia R, Pacheco J, Pacheco M, Benítez Read J S, López R, Plasma sources science and technology, **15**, 237 (2006).
[8].   Chang J. S, Urashima K, Tong Y, Journal of Electrostatics, **57**, 313 (2003).
[9].   Vacquié S, Sciences et techniques de l´ingénieur: L`arc électrique, Tome I, Editions EYROLLES, 2000, 238–247
[10].   PhysicsNIST,2010.http://physics.nist.gov/PhysRefData/ASD/lines_form.html
[11].   Restrepo E, Devia A, Revista colombiana de física, **34**, 748 (2002).
[12].   Valdivia R, Pacheco M, Pacheco J, Estrada N, Ramos F, García J, Freton P, International Conference on Phenomena in Ionized Gases, Cancún, México, 2009,
[13].   Manley T.C, Trans. Electrochem, **84**, 83 (1943).
[14].   Kogelschatz U, Plasma Chemistry and Plasma Processing, **23**, 1 (2002).
[15].   Deng Xu Tao, Kong Michel G, IEEE Transactions on plasma science, **32**, 1709 (2004).
[16].   Civitano L, Dinelli G, Busi F, Gallimberti M. R, IEEE Transactions on Plasma Science, **15**, 814 (2006).
[17].   Liu S, Neiger M, Journal of physics. D, Applied physics, **36**, 1565 (2003).
[18].   Fridman A, Plasma Chemistry, Cambridge University Prees, First published, 328 (2008).
[19].   Cormier J. M, GREMI Université d'Orléans, **130** 180 (2005).